16 Magnetism

Thomas Brückel, IFF, FZ-Jülich

16.1 Introduction

Magnetism is a very active and challenging subject of solid state science since it represents a typical many-body problem and a complex application of quantum-mechanics, statistical physics and electromagnetism. During the last decades, new discoveries have emerged in this field due to the synthesis of new classes of magnetic materials, due to improved or new powerful techniques or due to advancements in solid state theory. Let us mention a few examples of materials of current interest: the high temperature superconductors and the colossal magneto-resistance manganite compounds, both of which have structures derived from the perovskite structure, the rare-earth nickel-born carbide compounds with a coexistence of magnetism and superconductivity, the large class of Kondo systems and heavy fermion compounds, spin glasses and spin liquids or new and rather complex hard magnetic materials, just to mention a few. Besides bulk materials, magnetism of thin films and surfaces became a topic of great current interest, mainly due to the improved preparation techniques. Driven by pure curiosity, scientists have discovered many fundamental effects of thin film devices, such as the oscillating interlayer coupling or the giant magneto-resistance effects. Within less than ten years from their initial discovery, these effects found their applications for example in read heads of computer hard disks. A promising new field of application emerges, so-called magneto-electronics with spin transistors or magnetic random access memories MROM. This should serve us as an excellent example, how curiosity driven fundamental research can find new applications of an effect known since 2500 years (the discovery of the magnetism of magnetite) which are able to change our modern life. This progress is largely due to new experimental methods and again we just want to mention a few: developments in the field of polarised neutron scattering, such as the ^{3}He-polarisation filter or zero-field neutron polarimetry, the development of the spin resonance techniques, resonant nuclear scattering of synchrotron radiation or magnetic x-ray diffraction. Finally, all this experimental progress would be in vain without the improvements of the theory, which provide us with a deeper understanding of correlated electron systems. Probably the most powerful technique that has emerged during the last years is the density functional theory which allows one to calculate

the ground state of metallic magnets. Numerical methods such as Monte-Carlo simulation allows us to test models of complex disordered magnetic systems.

After having motivated the interest in solid state magnetism, let us come back to the basic magnetic properties. Quite generally, a magnetic system can be described by its magnetisation, which denotes the total magnetic moment per unit volume. The magnetisation of a sample can vary in space and time: $\underline{M}(\underline{r},t)$. The magnetisation is coupled to the conjugate magnetic field $\underline{H}(\underline{r},t)$. If the excitation $\underline{H}$ is very small, the response will, to a good approximation, be linear. In the framework of this linear response theory, we can define a magnetic susceptibility χ by:

$$\underline{M} = \underline{\underline{\chi}} \cdot \underline{H} \tag{16.1}$$

Here, $\underline{\underline{\chi}}$ is written as a tensor to describe anisotropic magnetic response. In isotropic systems, $\underline{M}$ will align parallel to $\underline{H}$ and χ reduces to a scalar quantity. More generally, for a spatially and temporally varying magnetic field, we can write:

$$\underline{M}(\underline{r},t) = \iint d^3r'\,dt'\,\underline{\underline{\chi}}(\underline{r}-\underline{r}',t-t')\cdot\underline{H}(\underline{r}',t') \tag{16.2}$$

Every material shows a magnetic response. Most materials are diamagnetic with a negative susceptibility χ, which expresses Lenz's rule that the induced magnetisation $\underline{M}$ is anti-parallel to the magnetic field H. Of greater interest are materials, in which χ is positive. Here, two classes of materials have to be distinguished: localised electron systems (e. g. ionic compounds) and itinerant electron systems (metals). Localised electron systems with $\chi > 0$ have open shells with unpaired electrons. Spin- S, orbital- L, and total- angular momentum J for the free ion are determined by Hund's rules. These values can be modified by solid state effects such as the crystalline field or spin transfer into covalent bonds. In itinerant electron systems, the conduction electrons carry the magnetic moment. Within a simple band picture, magnetism arises from an unequal population of spin-up and spin-down bands. At elevated temperatures, systems with $\chi > 0$ show paramagnetic behaviour with strongly fluctuating magnetic moments. As the temperature is lowered interaction between the moments becomes more and more important. In general magnetic dipole-dipole interactions play only a minor

role, compared to the stronger exchange interactions, which result from Coulomb interaction and the Pauli principle. In ionic compounds, we observe direct exchange, if the orbitals of two magnetic ions overlap or super-exchange and double exchange, if the interaction is mediated via an intervening anion. In itinerant electron systems, the interaction is mediated by the conduction electrons and has an oscillating character. This indirect coupling of magnetic moments by conduction electrons is referred to the Rudermann-Kittel-Kasaya-Yosida (RKKY) interaction. If the energy equivalent kT is in the order of the interaction energy, a phase transition from the paramagnetic high temperature state to a magnetically long-range ordered low temperature state can eventually take place. Systems with spontaneous macroscopic magnetisations such as ferromagnets (FM) and ferrimagnets have to be distinguished from antiferromagnets (AF), for which the zero-field magnetisation vanishes. The microscopic arrangement of spin- and orbital- magnetic moments, the so-called magnetic structure, can be rather complex, especially in the case of antiferromagnets.

Neutron scattering is a most powerful technique for the investigation of magnetism due to the magnetic dipole interaction between the magnetic moments of the electrons in the sample and the nuclear magnetic moment of the neutron. We have seen in chapter 3 that for elastic events, the neutron scattering cross section is directly related to the Fourier transform of the magnetic moment density distribution. For the inelastic case, one can show that the double differential cross section for magnetic neutron scattering is connected with the most fundamental quantity, the Fourier transform of the linear response function or susceptibility (16.2) $\chi(\underline{r},t)$ in microscopic space and time variables $\underline{r}$ and t, respectively. In contrast to macroscopic methods it allows one to study magnetic structures, fluctuations and excitations with a spatial and energy resolution well adapted to atomic dimensions. Traditionally neutron scattering is the method to study magnetism on an atomic level, only recently complemented by the new technique of magnetic x-ray scattering.

In what follows, we will give a few examples for applications of neutron scattering in magnetism. Obviously it is completely impossible to give an representative overview within the limited time, nor is it possible to reproduce the full formalism. Therefore we will just quote a few results and concentrate on the most simple examples. Even so polarisation analysis experiments are extremely important in the field, we will not discuss these rather complex experiments and refer to chapter 4.

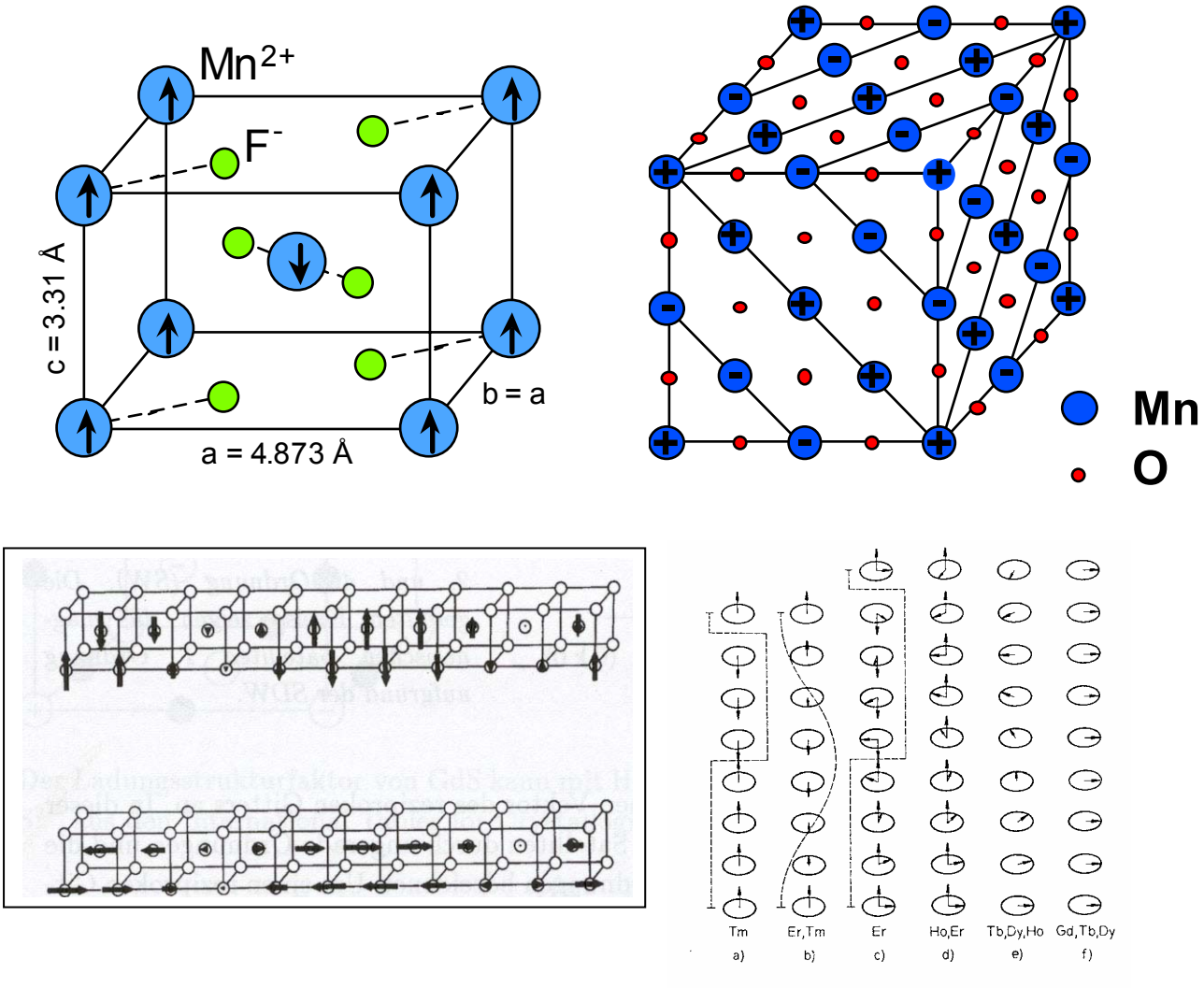

Fig. 16.1: Some examples of magnetic structures: a) The collinear antiferromagnetic structure of MnF_2. The spin moments at the corners of the tetragonal unit cell point along the c-direction, the spin moment in the centre of the unit cell is antiparallel to the moments at the corners. b) The MnO-type magnetic structure on a fcc lattice. Spins within 111 planes are parallel, adjacent planes are coupled antiferromagnetically. c) The spin density wave of chromium, which can be described by an amplitude variation along one of the cubic 001 axis. The spin density wave can be longitudinal or transversally polarised. d) Schematic representation of the magnetic structures of the hexagonal rare-earth metals. Spins in the hexagonal basal plane are always parallel. The figure shows, how successive planes along the c-directions are coupled. One can distinguish a simple ferromagnetic phase, a c-axis modulated phase, helix and cone phases. In reality, the magnetic structures are much more complex with spin slip or multi-k structures. A recent review is given by [1].

16.2 Magnetic Structure Determination

As mentioned in the introduction, the magnetic structure of a substance exhibiting magnetic long range order can be very complex. In general a magnetic structure can be described by its Fourier-components in the form

$$\underline{m}_{l,j} = \sum_{\underline{q}} \underline{m}_{\underline{q}j} \cdot \exp\left(-i\underline{q} \cdot \underline{R}_l\right) \tag{16.3}$$

where $\underline{m}_{l,j}$ denotes the moment of atom j in cell l and $\underline{q}$ is the so called magnetic propagation vector. Some examples for magnetic structures are given in figure 16.1.

Magnetic neutron scattering is the classical method to determine magnetic structures. As neutral particles, neutrons penetrate deep into most materials and allow to study bulk properties. Thermal neutrons have wavelengths in the vicinity of 1 Å, which is well adapted to studies with atomic resolution. Neutrons carry a magnetic dipole moment

$$\underline{\mu}_n = -\gamma\mu_N \cdot \underline{\sigma} \tag{16.4}$$

with the gyromagnetic ratio $\gamma = -1.913$ of the neutron and the nuclear magneton $\mu_N = 5.051 \cdot 10^{-27}\,\mathrm{J/T}$. This magnetic moment of the neutron can interact with the magnetic field created by the spin or orbital angular momentum of unpaired electrons within the solid, see chapter 3. If we restrict ourselves to elastic scattering of unpolarised neutrons, the purely magnetic scattering cross section is given by

$$\left(\frac{d\sigma}{d\Omega}\right)_{el,mag} = \left(\frac{\gamma r_0}{2}\right)^2 \left|\left\langle M_\perp(\underline{Q})/\mu_B \right\rangle\right|^2 = \left(\frac{\gamma r_0}{2}\right)^2 \left|\left\langle 2S_\perp(\underline{Q}) + L_\perp(\underline{Q})\right\rangle\right|^2 \tag{16.5}$$

with $\frac{\gamma r_0}{2} = 2.696\ \mathrm{fm}$. $\mathrm{M}_\perp(\underline{\mathrm{Q}})$ is the component of the Fourier transform of the sample magnetisation perpendicular to the scattering vector. $\underline{\mathrm{S}}(\underline{\mathrm{Q}})$ and $\underline{\mathrm{L}}(\underline{\mathrm{Q}})$ are the Fourier transform of the spin- and orbital- angular momentum density, respectively. The index $\perp$ denotes the component of the corresponding quantity perpendicular to the scattering vector. Neutrons

only "see" this component and not the component of the magnetisation along the scattering vector Q (compare chapter 3). This directional dependence allows one to determine the spin direction, while the magnetic propagation vector can be determined from the position of the magnetic Bragg reflections. Finally, the magnitude of the magnetic moment can be determined by comparing the intensities of the magnetic Bragg reflections with the intensities of nuclear reflections. The scattering amplitude of neutrons by a single fixed nucleus is given by the scattering lengths tabulated in [2]. As an example, the scattering length for cobalt amounts to 2.49 fm, which is comparable to the equivalent magnetic scattering amplitude for spin = 1/2 of 2.696 fm. The formalism for magnetic neutron scattering is detailed by Squires [3] and Lovesey [4], the determination of magnetic structures is described by Rossat-Mignod [5].

Here we want to discuss the most simple example, the determination of the magnetic structure of MnF_2. For simplicity, we will neglect the scattering of the fluorine atoms completely. Then our problem reduces to magnetic Bragg diffraction from a tetragonal body centred antiferromagnet. In the so called antiferromagnetic order of type I, shown in figure 16.2, all spins at the corners of the unit cell are parallel, while the spin in the centre is anti-parallel to the spins at the corners. We assume that due to some anisotropy, e.g. the crystal field effects, all moments are aligned along ±c.

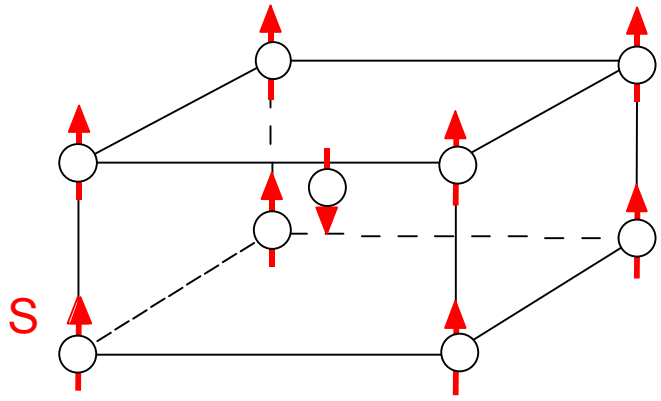

Fig. 16.2: Magnetic structure of a type I antiferromagnet on a body-centred tetragonal lattice. In the figure is assumed that c is the easy axis, i.e. all spins are aligned along c.

The scattering power density can be calculated as a convolution of an infinite three dimensional lattice, which describes the position of the origin of all unit cells, with the scattering power density of a pair of atoms located at the origin and at the centre of the unit cell. Therefore, when calculating the scattered intensity as the Fourier transform of the scattering power density, it is given as a product of the Fourier transform of the lattice and the Fourier transform of the scattering power density of a pair of atoms. The Fourier transform of the lattice is the well known Laue function (compare chapter 3). It gives rise to the Bragg reflections at integer h, k, l. The intensity of these Bragg reflections is being modulated by the Fourier transform of the scattering power density within the unit cell (here of the atom pair), the so called *elastic structure factor*. The structure factor for the pure nuclear scattering is given by:

$$\begin{aligned} S_N(h,k,l) &= b(1+e^{2\pi i(h\cdot\frac{1}{2}+k\cdot\frac{1}{2}+l\cdot\frac{1}{2})}) \\ &= b(1+(-1)^{h+k+l}) = \begin{cases} 0 & h+k+l \quad uneven \\ 2b & h+k+l \quad even \end{cases} \end{aligned} \tag{16.6}$$

The body centring gives rise to an extinction of all reflections with index h+k+l uneven, while all reflections with h+k+l even have the same intensity. In complete analogy to (16.6), the magnetic structure factor can be calculated. We only have to take into account that the spin direction in the centre is opposite to the spin directions at the corners, which can be described by a different sign for the two spins:

$$\begin{aligned} S_M(h,k,l) &= \gamma_n r_o f_m S(1-e^{2\pi i(h\cdot\frac{1}{2}+k\cdot\frac{1}{2}+l\cdot\frac{1}{2})}) \\ &= \gamma_n r_o f_m S(1-(-1)^{h+k+l}) = \begin{cases} 2\gamma_n r_o f_m S & h+k+l \; uneven. \\ 0 & h+k+l \; even \end{cases} \end{aligned} \tag{16.7}$$

The magnetic structure is „anti body centred“: all reflections with index h+k+l even vanish, while reflections with h+k+l uneven are present. In the diffraction pattern, a magnetic Bragg reflection appears right between two nuclear ones. The intensity of the magnetic reflections decreases with increasing momentum transfer due to the magnetic form factor (see chapter 3), while the nuclear reflections have constant intensity, if we neglect the temperature factor – see figure 16.3.

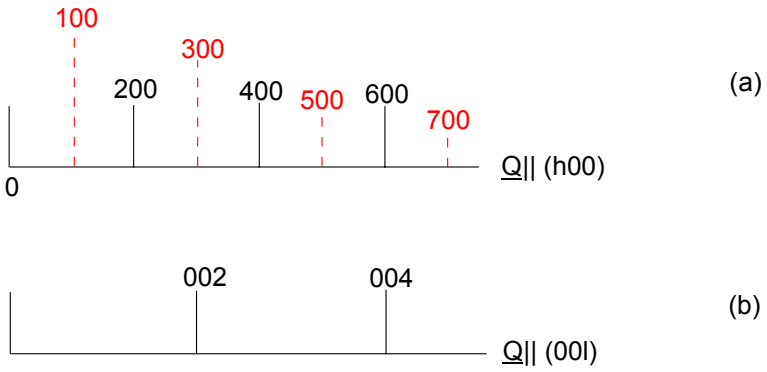

Fig. 16.3: Schematic plot of a neutron diffraction diagram for the antiferromagnet of fig. 16.2. Top: along the (h00) direction; bottom: along (00l). Magnetic Bragg reflections are indicated by the broken lines. The height of the lines is representative for the scattered intensity.

We can determine the direction of the magnetic moments with the help of the directional factor in eq. (16.5). If one measures along the tetragonal a or b directions, one obtains the magnetic Bragg reflections of figure 16.3 a. However, if one measures along c, S || Q holds, i.e. all magnetic reflections of type 0 0 l are extinct and one obtains the diffraction pattern depicted in figure 16.3 b. In this simple case, one can directly deduce the spin direction along c from the extinction of the 0 0 l reflections. Finally one can obtain the magnitude of the spin moment by comparing the intensities of the magnetic Bragg reflections with the intensities of the nuclear ones.

16.3 Magnetic Form Factors; Magnetisation Densities

For the magnetic structure determination we used a predetermined form factor, e.g. from Hartree-Fock calculations of electronic wave functions for the free atom [6]. Each atomic site was characterised by just one integral variable, the atomic magnetic moment. A scattering experiment can, however, give much more information, if sufficient Fourier components can be measured. We can then obtain the magnetisation density within each atom, which will show deviations from the density of the free atom due to solid state effects. Magnetisation density can be transferred to neighbouring atoms by covalent bonds. In metallic magnetic systems, the "magnetic" electrons are itinerant and the magnetisation density is strongly de-localised. We learned in chapter 3 that the magnetic form factor is the Fourier transform of

the magnetisation density of one atom. Therefore magnetic form factor measurements give us all the important information about such solid state effects.

To illustrate the kind of information we can obtain from such measurements let us quote some recent studies of high temperature superconductors or molecular magnets. There are theories of high temperature superconductivity, which propose a magnetic coupling mechanism for the Cooper-pairs. While no long range ordered magnetic structure is observed in the super-conducting state, dynamic magnetic fluctuations have been searched for with neutron scattering [7,8]. If one wants to detect, which atomic sites are susceptible to magnetism, one can study the magnetisation density induced in the material by an external magnetic field [9]. Molecular magnets are another active field of current interest, due to their very high potential for applications, but also due to fundamental interest. These are organic compounds, where the magnetism is not due to intra-atomic exchange ("Hund's rules"), as in the case of 3d or 4f metal ions, but due to the specific arrangement of bonds. The magnetisation density is distributed over many atomic sites. A neutron study of it's distribution can give us insight to the mechanism giving rise to the magnetic coupling and thus guide us in the search for new, optimised materials [10].

The most efficient way to measure weak magnetic signals is to use the interference between magnetic and nuclear scattering. Using this interference effect, we can even determine the phase of the magnetic structure factors, in addition to their magnitude. In this special case we have then solved the phase problem of crystallography.

We have learned in chapter 4 that this interference term can only be measured with polarised neutrons and cancels for unpolarised neutron diffraction. An interference between nuclear and magnetic scattering can only occur, if both types of scattering are allowed, i.e. the interference can only appear in the "non-spin flip" channel, if the nuclear as well as the magnetic structure factor are non- vanishing. To maximise the magnetic signal, one chooses a diffraction geometry as in figure 16.4, for which the magnetisation is perpendicular to the diffraction plane. This condition can be enforced by applying a strong magnetic field along this direction.

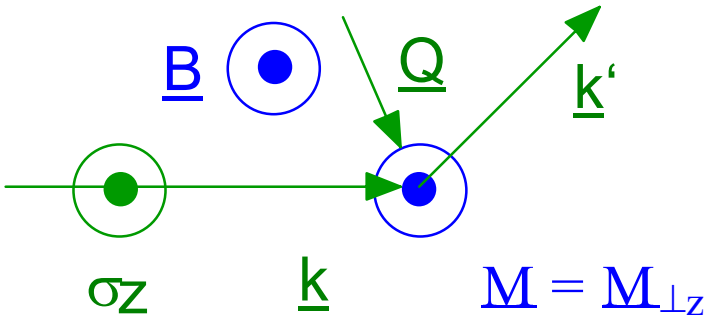

Fig. 16.4: Scattering geometry for measuring the interference term between nuclear- and magnetic scattering with polarised neutrons, but without polarisation analysis.

The relevant cross sections to measure the interference term in this geometry are:

$$\left(\frac{d\sigma}{d\Omega}\right)_{++} = \left| b(\underline{Q}) - \frac{\gamma_n r_o}{2\mu_B} M(\underline{Q}) \right|^2 = b^2 - 2\frac{\gamma_n r_o}{2\mu_B} bM + \left(\frac{\gamma_n r_o}{2\mu_B}\right)^2 M^2 \qquad (16.8)$$

b,M real

$$\left(\frac{d\sigma}{d\Omega}\right)_{--} = \left| b(\underline{Q}) + \frac{\gamma_n r_o}{2\mu_B} M(\underline{Q}) \right|^2 = b^2 + 2\frac{\gamma_n r_o}{2\mu_B} bM + \left(\frac{\gamma_n r_o}{2\mu_B}\right)^2 M^2 \qquad (16.9)$$

Besides the magnitude square of the amplitude for nuclear- and magnetic- scattering, respectively, these cross sections contain one term, in which a product of the magnetic- and nuclear- amplitudes appears. This interference term is especially useful, if the amplitude of magnetic scattering is much smaller than the amplitude of nuclear scattering:

$$\left| \frac{\gamma_n r_o}{2\mu_B} M \right| << |b| \qquad (16.10)$$

This is for example the case, if an external magnetic field induces a weak magnetisation in the paramagnetic state, when the ration between magnetic- and nuclear- amplitude is often below 10^{-3}. This implies that the contribution from magnetic scattering to the total signal is in the order of 10^{-6} or less, and thus no longer measurable. However, if we take data in two measurements, once with the neutron polarisation parallel and once anti-parallel to the magnetic field, we can determine the so-called *flipping ratio*:

$$R(\underline{Q}) = \frac{(d\sigma/d\Omega)_{++}}{(d\sigma/d\Omega)_{--}} = \frac{1 - \frac{\gamma_n r_o}{\mu_B}\frac{M}{b} + \ldots}{1 + \frac{\gamma_n r_o}{\mu_B}\frac{M}{b} + \ldots} \approx 1 - 4\frac{\gamma_n r_o}{2\mu_B}\frac{M(\underline{Q})}{b(\underline{Q})} \qquad (16.11)$$

Note that the polarisation of the scattered beam is known a priori (only non-spin flip processes can occur), so that the experiment is being done with a polarised beam, but without polarisation analysis. The flipping ration (16.11) depends linearly on the magnetic structure factor, instead of quadratic as the scattered intensity. Therefore much smaller values of the magnetic structure factor can be determined. If the nuclear structure factor is known (e.g. from a prior neutron diffraction experiment), these measurements of the flipping ratio give access to a highly precise determination of the phase and magnitude of the magnetic structure factor.

An example is given by the measurement of the form factor of chromium. Cr is the archetypal itinerant antiferromagnet. Therefore the magnetisation density is very de-localised. As a consequence, the magnetic form factor drops extremely rapidly with increasing momentum transfer. In a recent synchrotron x-ray experiment, we could demonstrate that this form factor is spin only [11]. However, in a polarised neutron diffraction experiment we could show [12], that a magnetisation induced in the paramagnetic state by an external magnetic field is much more localised around the individual atoms. Therefore, the field-induced form factor decreases much slower, compare figure 16.6. It has a large contribution (60 %) of orbital angular momentum, quite in contrast to the form factor in the ordered state. By means of a Fourier transform or with the so-called *Maximum Entropy Method* a magnetisation density distribution within the unit cell can be reconstructed (compare figure 16.7). Such data are of utmost importance to test and improve modern band theories, such as the fully relativistic *density functional theory* and thus to obtain a better understanding of the metallic state.

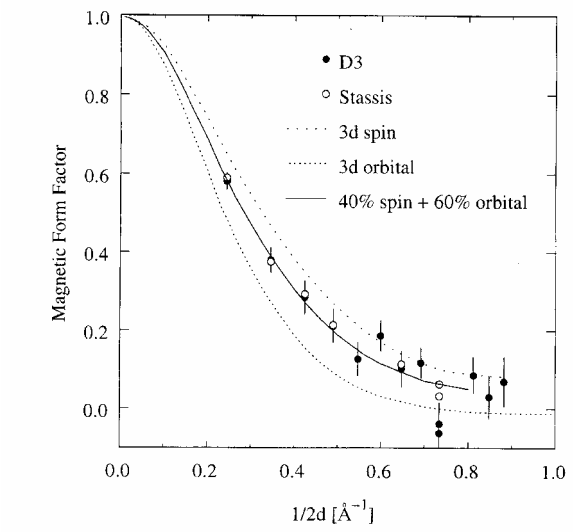

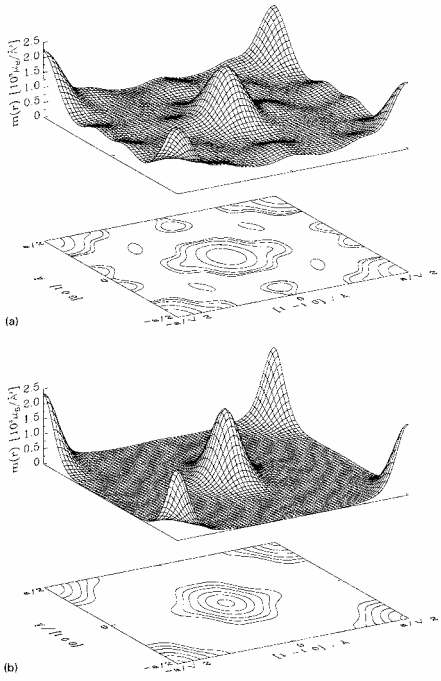

Fig. 16.6: Induced magnetic form factor of Cr for a field of 4.6 T. Open and filled circles are experimental values, the Lines are calculations for spin-, Orbital- and total moment.

Fig. 16.7: Projection of the induced magnetisation density distribution onto the <110> plane. above: Fourier transform Below: Maximum entropy reconstruction

16.4 Magnetic Phase Transitions

Phase transitions can occur between different magnetic phases as a function of various thermodynamic parameters, such as magnetic field, temperature or pressure. Here we will restrict ourselves to the most simple case of a transition from a low temperature ferromagnetic (FM) or antiferromagnetic (AF) phase to a high temperature paramagnetic (PM) phase. First, we will discuss this phenomenon qualitatively, then introduce the quantitative description and finally show just one example of a neutron diffraction study.

The magnetic long range order discussed in section 16.2 can only be stable, as long as the thermal energy k_BT is small enough compared to the exchange interactions giving rise to magnetic order. At sufficiently high temperatures, entropy wins and the magnetic moments

fluctuate in space and time. A phase transition has occurred at a critical temperature, called *Curie temperature* T_C for ferromagnets or *Néel temperature* T_N for antiferromagnets, from a long range ordered state at low temperatures to a paramagnetic high temperature phase. The two phases are characterised by an *order parameter*, such as the magnetisation for ferromagnets or the sublattice magnetisation for antiferromagnets. In the paramagnetic phase this order parameter vanishes, while in the low temperature phase it increases towards a saturation value, when the temperature is lowered. Depending on whether the order parameter changes discontinuously or continuously at the critical temperature, the phase transition is of *first-* or *second- order*, respectively. At least for local moment systems, the magnetic interactions and moments are still present in the paramagnetic phase. Therefore above the critical temperature, magnetic correlations persist. This magnetic short range order fluctuates in time and extends over regions with characteristic linear dimensions, called the *correlation length*. When we decrease the temperature in the paramagnetic phase towards the transition temperature, the correlation length increases. Larger and larger regions develop which show short range order characteristic for the low temperature phase. The larger these correlated regions, the slower the fluctuation-dynamics. At the critical temperature of a second order phase transition, the correlation length and the magnetic susceptibility diverges, while the dynamics exhibits a critical slowing down.

Besides the magnetic phase transitions, there exist also structural phase transitions. However, experiments on magnetic model systems provided the basis for our modern understanding of this complex co-operative effect. Th reason is that magnetic model systems can often be described by some very simple Hamiltonian, such as the Heisenberg (16.12), the x-y (16.13) or the Ising model (16.14), depending whether the system is isotropic, has a strong planar- or a strong uniaxial anisotropy, respectively:

Heisenberg: $$H = \sum_{i,j} J_{ij} \underline{S}_i \cdot \underline{S}_j \tag{16.12}$$

x-y: $$H = \sum_{i,j} J_{ij} \left(S_{ix} S_{jx} + S_{iy} S_{jy} \right) \tag{16.13}$$

Ising: $$H = \sum_{ij} J_{ij} S_{iz} S_{jz} \tag{16.14}$$

Here, J_{ij} denotes the exchange constant between atoms i and j, $S_{i\alpha}$ is the component α (=x, y or z) of the spin operator $\underline{S}_i$ of atom i. If the Hamiltonian depends on three- (Heisenberg-model, 16.12), two- (x-y-model, 16.13) or one- (Ising-model, 16.14) components of the spin operator, one can define a three-, two- or one dimensional order parameter. Moreover, there are crystal structures, where the magnetic atoms are aligned along well separated chains or planes, so that besides the usual three dimensional lattice, there exist magnetic model systems in one and two space dimensions. Finally, depending on whether the system shows covalent or metallic bonding, the exchange interactions can be short- or long ranged, respectively.

The experimental investigation of continuous (second order) phase transitions in many magnetic model systems revealed a quite surprising behaviour in a critical region (a temperature range around the ordering temperature with a width of by and large 10 % of the ordering temperature) close to the phase transition: independent of the precise nature of the system under investigation, the phase transition shows universal behaviour. These experimental results laid the foundations for the formulation of a modern theory of second order phase transitions, the *renormalisation group theory*.

If we define a *reduced temperature* as

$$\tau = \frac{T - T_C}{T_C} \tag{16.15}$$

then all relevant thermodynamical parameters show a power-law behaviour close to the second order phase transition:

specific heat:	$c_H \propto \tau^{-\alpha}$	(16.16)
order parameter ($T<T_C$):	$m \propto (-\tau)^{\beta}$	(16.17)
susceptibility:	$\chi \propto \tau^{-\gamma}$	(16.18)
correlation length:	$\xi \propto \tau^{-\nu}$	(16.19)

The surprising discovery was that all systems can be classified into *universality classes*. Within a given universality class, the values of the *critical exponents* α, β, γ and ν are the

same and do not depend on the detailed nature of the system. Moreover, the critical exponents for a given system are not independent, but fulfil certain *scaling relations*, see e.g. [13]. To which universality class a system belongs is determined by three criteria:

Dimensionality of the order parameter n

Space dimensionality d

Range of the interactions (long- or short ranged)

Table 16.1 lists values of the critical exponents for some universality classes.

n	1	1	2	3
d	2	3	3	3
α	0	0.106	-0.01	-0.121
β	0.125	0.326	0.345	0.367
γ	1.75	1.238	1.316	1.388
ν	1	0.631	0.669	0.707

Tab. 16.1: Values of the critical exponents for a few universality classes according to [13].

As an example we have selected a rather unusual magnetic phase transition, which turns out to be of first order (discontinuous) and thus cannot be classified by the above criteria. Let us briefly discuss the AF-PM phase transition of MnS_2 [14].

The magnetic semiconductor MnS_2 orders with the type-III antiferromagnetic structure on the fcc lattice with the wave vector $\underline{q}$=(1,1/2,0) (compare (16.3)). The antiferromagnetic phase transition at T_N = 48.2 K is found to be of first order, quite in contrast to the classical behaviour for such a compound. We performed a neutron scattering study in a search for the driving mechanism. Figure 16.8 shows a contour plot of the magnetic diffuse scattering in the (001) plane in the paramagnetic phase about 17K above T_N. One can clearly see, how the magnetic diffuse scattering is concentrated at the positions (1,1/2,0), (1,3/2,0), (3/2,1,0) etc, where in the long range ordered phase the magnetic Bragg reflections appear. However, a closer examination shows that the positions at which the diffuse scattering is centred, are not the rational positions listed above.

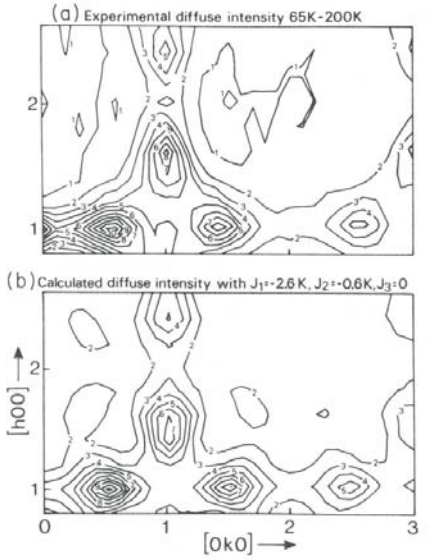

Fig. 16.8: Contour plot of the magnetic diffuse scattering intensity of MnS_2 in the (001) plane at 65 K. Above: measurement; below: calculation

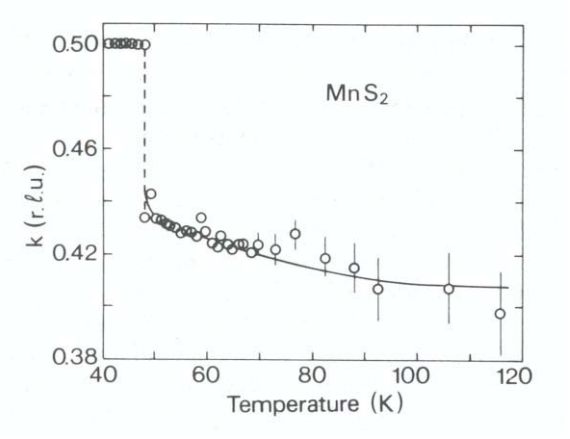

Fig. 16.9: Temperature variation of the incommensurate component.

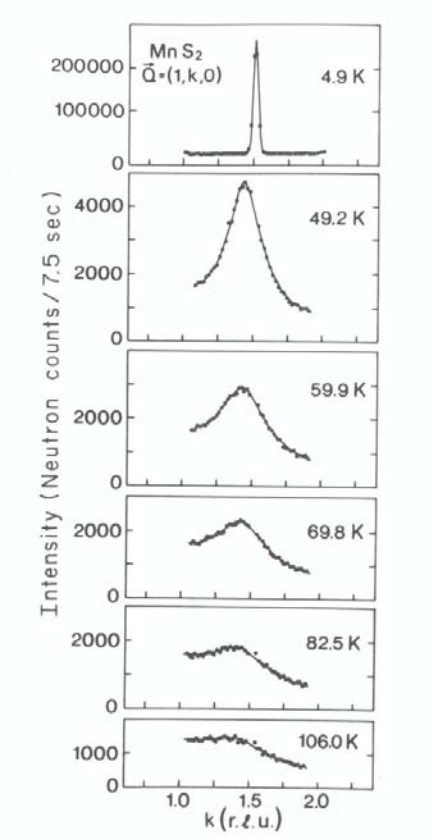

Fig. 16.10: Magnetic diffuse neutron scattering of MnS_2 in reciprocal lattice scans parallel to the modulation vector.

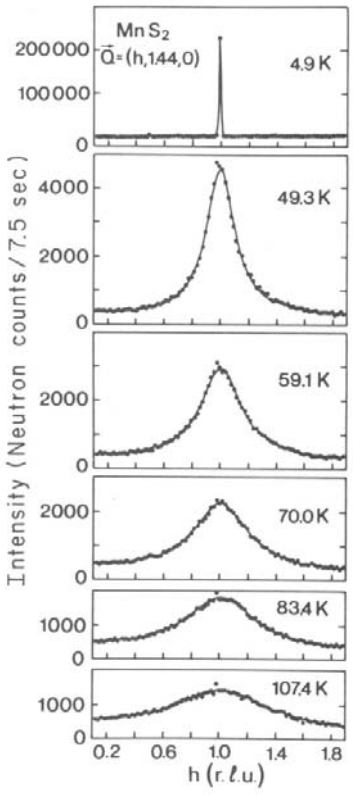

Fig. 16.11: Magnetic diffuse neutron scattering of MnS_2 in reciprocal lattice scans perpendicular to the modulation vector.

Figures 16.10 and 16.11 show the magnetic diffuse neutron scattering of MnS_2 at different temperatures above T_N and the magnetic Bragg peak at 4.9 K (topmost figure). We can clearly observe, how with decreasing temperature the diffuse scattering becomes sharper in reciprocal space and how the peak intensity increases strongly. However, for scans along (1,k,0) the diffuse scattering is not centred at the low temperature Bragg position, while it is centred for the perpendicular scans in the (h,k,0) plane. The magnetic short range order is "*incommensurate*" with the lattice. This means that the periodicity observed in the diffuse magnetic scattering is not just a simple rational multiple of the chemical unit cell periodicity. Figure 16.9 shows the temperature variation of the incommensurate component of the vector at which the diffuse scattering is centred. Note the jump characteristic for a first order transition. Figure 16.9 demonstrates that we can understand the paramagnetic-antiferromagnetic phase transition in MnS_2 as a transition from incommensurate short range order to commensurate long range order. Now it is well established that such "*lock-in-transitions*" are of first order, which explains the unusual behaviour of MnS_2. The problem remains which interaction leads to the shift of the diffuse peak as compared to the Bragg reflection. This question can be solved with model calculations, such as the ones depicted in figure 16.8 [14]. It turns out that an anisotropy term in the Hamiltonian can give rise to the observed effect.

Finally we want to show an example for a true "classical" second order transition, the PM-AF transition in MnF_2. In this case, we have performed the measurements with high energy synchrotron x-rays due to the better reciprocal space resolution as compared to neutrons [15]. Figure 16.12 shows a double logarithmic plot of the reduced sublattice magnetisation m ($m = M/M_S$, where M_S is the saturation value of the magnetisation) versus the reduces temperature τ, defined in eq. (16.15). In this plot, the data points nicely line up along a straight line, corresponding to a power law behaviour as expected from (16.7). The critical exponent β of the sub-lattice magnetisation can be obtained to great precision: $\beta = 0.333\ (3)$, corresponding roughly to the exponent expected for an Ising system (n=1, d=3) according to table 16.1. However, the calculated and measured value do not quite coincide, at least to within two standard deviations, which demonstrates that the precise values of the critical exponents are still not very well established.

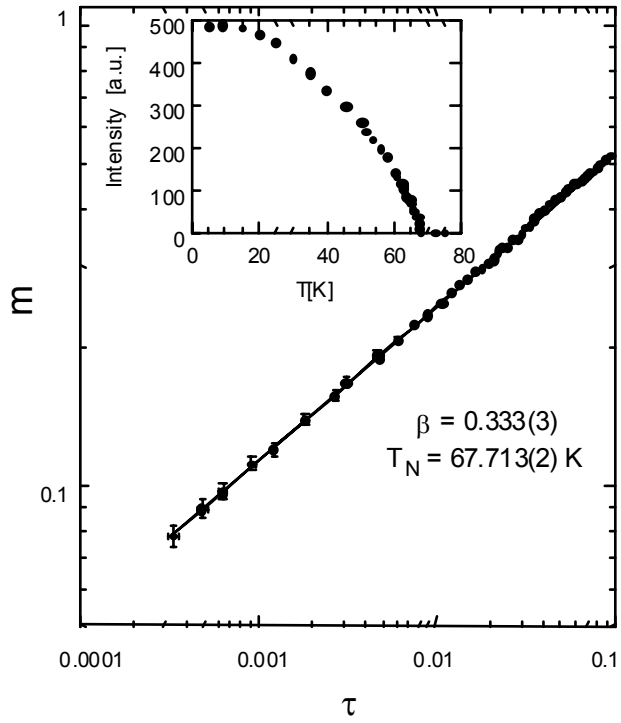

Fig. 16.12: Magnetic Bragg diffraction from MnF_2. The inset shows the temperature dependence of the intensity of the magnetic 300 reflection from 5 to 80K. In the main graph is plotted the reduced sub-lattice magnetisation as a function of reduced temperature on a double logarithmic scale together with a fit employing a power-law function.

16.5 Summary

We have given a few examples of the applications of neutron scattering in magnetism. We have seen how neutrons can be used to investigate the magnetisation density distribution on an atomic level. Besides the rather new technique of magnetic x-ray scattering, no other method can provide the same information on magnetic structure and magnetisation density. Neutrons are ideally suited to study magnetic phase transitions, which are model examples of co-operative phenomena in many body systems. Unfortunately, we were not able to cover other subjects, such as the important fields of magnetic excitations or thin film magnetism. Neutron scattering is the technique to measure spin wave dispersion relations used to determine magnetic interaction parameters (exchange interaction, anisotropy) – see chapter on excitations. In itinerant systems, the transition from collective spin wave like excitations to single particle like "Stoner" excitations could be observed with neutrons. Currently, more "exotic" excitations are in the centre of attention, such as the "resonance peak" in high

temperature superconductors, or excitations in low dimensional magnets. Finally, thin film magnetism is of high current interest due to it's applications in "magnetoelectronics". In this field, neutrons provide the crucial information about the magnetic structure and morphology of thin film devices, compare chapter on reflectometry. While we could not give a comprehensive review, the Jülich group is active in all these fields and we refer to our web page [16] for further information.

References

[1] J. Jensen & A. R. Mackintosh, "Rare Earth Magnetism", Clarendon Press, Oxford (1991)

[2] V. F. Sears, Neutron News 3 (1992) 26

[3] G. L. Squires, "Thermal Neutron Scattering", Cambridge University Press, Cambridge (1978)

[4] S. W. Lovesey, "Theory of Neutron Scattering from Condensed Matter", Clarendon Press, Oxford (1987)

[5] J. Rossat-Mignod, "Magnetic Structures" in: K. Sköld, D. L. Price: "Neutron Scattering", Academic Press, New York (1987)

[6] A. J. Freeman & R. E. Watson, Acta Cryst. 14 (1961), 231

[7] Th. Brückel, H.Capellmann, W. Just, O. Schärpf, S. Kemmler-Sack, R. Kiemel & W. Schäfer; Europhysics Letters 4 (1987) 1189

[8] B. Keimer et al, Physica B 234-236 (1997), 821

[9] J.X. Boucherle et al; Physica B192 (1993), 25

[10] Y.Pontillon et al, Physica B 267-268 (1999), 51

[11] J. Strempfer, Th. Brückel, W. Caliebe, A. Vernes, H. Ebert, W. Prandl & J.R. Schneider; Eur. Phys. J. B14 (2000), 63

[12] J. Strempfer, Th. Brückel, G. J. McIntyre, F. Tasset, Th. Zeiske, K. Burger, W. Prandl, Physica B 267 - 268 (1999), 56

[13] M.F. Collins "Magnetic Critical Scattering", Oxford University Press, Oxford 1989

[14] T. Chattopadhyay, Th. Brückel & P. Burlet; Phys. Rev. B44 (1991), 7394

[15] J. Strempfer, Th. Brückel, U. Rütt, J.R. Schneider, K.-D. Liss & Th. Tschentscher; Acta Cryst. A52 (1996), 438

[16] http://www.fz-juelich.de/iff/Institute/ism/